PHYSICAL REVIEW B VOLUME 34, NUMBER 4 15 AUGUST 1986

Angle-resolved photoelectron-spectroscopy study of the Si(111) $\sqrt{3}\times\sqrt{3}$-Sn surface: Comparison with Si(111) $\sqrt{3}\times\sqrt{3}$-Al, -Ga, and -In surfaces

T. Kinoshita, S. Kono, and T. Sagawa
Department of Physics, Faculty of Science, Tohoku University, Sendai 980, Japan
(Received 14 May 1986)

Angle-resolved ultraviolet photoelectron spectra have been measured for the Si(111) $\sqrt{3}\times\sqrt{3}$-Sn surface. It has been found that the surface-state dispersions are very similar to those reported for the Si(111) $\sqrt{3}\times\sqrt{3}$-Al, -Ga, and -In (column-III metals) surfaces except for the presence of an additional metallic surface state. The metallic state observed for the $\sqrt{3}\times\sqrt{3}$-Sn surface seems to correspond to the otherwise unoccupied surface state for the $\sqrt{3}\times\sqrt{3}$-M (M = Al, Ga, In) surfaces. This suggests that the surface atomic geometry of the $\sqrt{3}\times\sqrt{3}$-Sn is essentially the same as those of the $\sqrt{3}\times\sqrt{3}$-M surfaces, in which a metal atom is situated in every $\sqrt{3}\times\sqrt{3}$ threefold-hollow site.

It is known that metal overlayers in submonolayer ranges on semiconductor surfaces cause surface superstructures with a variety of phases. It is expected that the study of the smallest surface superstructures of these submonolayer interfaces can give a basis for the understanding of the semiconductor surface reconstructions. Recently, electronic structures of Si(111) $\sqrt{3}\times\sqrt{3}$-Al,[1,2] -Ga,[3] and -In (Refs. 4–6) surfaces have been studied by angle-resolved ultraviolet photoelectron spectroscopy (ARUPS). It became clear from these studies that the surface electronic structures of the $\sqrt{3}\times\sqrt{3}$-M [abbreviation for the Si(111) $\sqrt{3}\times\sqrt{3}$-Al, -Ga, and -In surfaces where M = Al, Ga, In] are very similar to each other. The dispersions of the surface-state (SS) bands are in qualitative agreement with theoretical calculations of Refs. 4, 5, 7, and 8 for the threefold-hollow adatom models. This indicates that the atomic geometry of these three $\sqrt{3}\times\sqrt{3}$-M surfaces is essentially the same to each other and is the T_4 or H_3 structure.[4,5,7]

The first work on Sn (column-IV element) submonolayer overlayers on the Si(111) surface was the low-energy electron diffraction (LEED) study of Estrup and Morrison.[9] They found two kinds of $\sqrt{3}\times\sqrt{3}$ and a $2\sqrt{3}\times2\sqrt{3}$ phase depending on the Sn coverage and substrate temperature. Ichikawa recently reported a detailed study of the Sn-Si(111) system.[10] He observed $\sqrt{3}\times\sqrt{3}$, $2\sqrt{3}\times2\sqrt{3}$, and three large superstructures ($\sqrt{133}\times4\sqrt{3}$, $3\sqrt{7}\times3\sqrt{7}$, and $2\sqrt{91}\times2\sqrt{91}$) by reflection high-energy electron diffraction (RHEED). Yabuuchi performed a structural analysis for the Sn-Si(111) system by LEED and ion-scattering spectroscopy (ISS).[11] From these studies, it is now known that the Si(111) $\sqrt{3}\times\sqrt{3}$-Sn surface is formed at about the same coverage [$\sim\frac{1}{3}$ monolayer (ML); 1 ML being the surface atom density of the truncated Si(111) 1×1 surface] as the $\sqrt{3}\times\sqrt{3}$-M metal overlayer surfaces. Therefore, it is of great interest to know how the electronic structure of the $\sqrt{3}\times\sqrt{3}$-Sn surface differs from those of the $\sqrt{3}\times\sqrt{3}$-M surfaces. In this Rapid Communication, ARUPS measurement of the Si(111) $\sqrt{3}\times\sqrt{3}$-Sn surface is reported and compared with those of the $\sqrt{3}\times\sqrt{3}$-M surfaces.

The experiment was carried out in the same way as in previous studies[1,3] except for the evaporation of Sn atoms. 99.999% pure Sn was deposited from a Mo spiral basket onto a clean Si(111) 7×7 substrate at room temperature under a pressure of $\lesssim2\times10^{-10}$ Torr. Auger electron spectra showed no contaminants before and after the experiments. After heating the substrate, RHEED patterns showed $\sqrt{3}\times\sqrt{3}$ and/or $2\sqrt{3}\times2\sqrt{3}$ structures depending on the conditions of coverage and heating temperature in accordance with Ref. 10. The well-ordered $\sqrt{3}\times\sqrt{3}$ surface for the ARUPS measurement was obtained by deposition of $\sim\frac{1}{3}$ ML Sn and $\sim430\,^{\circ}$C heating.

Some of the observed ARUPS spectra of Si(111) $\sqrt{3}\times\sqrt{3}$-Sn surface are shown in Fig. 1, where the polar angles of electron emission are changed along $\bar{\Gamma}$-$\bar{M}$-$\bar{\Gamma}$ and $\bar{\Gamma}$-$\bar{K}$-$\bar{M}$ directions of the $\sqrt{3}\times\sqrt{3}$ surface Brillouin zone (SBZ). The SS peaks are marked with bars and named S_1, S_1', S_2, and S_3. The distinction of these SS peaks is described later. Figure 2 shows the diagram of the binding energy (E_b) plotted against the electron wave vector ($k_\parallel$) parallel to the surface for the $\sqrt{3}\times\sqrt{3}$-Sn surface (filled symbols) along the $\bar{\Gamma}$-$\bar{M}$-$\bar{\Gamma}$ direction, which is converted from the actual spectra in Fig. 1 and others not shown here. Figure 3 is the diagram along the $\bar{\Gamma}$-$\bar{K}$-$\bar{M}$ direction. In Figs. 2 and 3, the diagrams for the $\sqrt{3}\times\sqrt{3}$-Ga surface[3] (open symbols) along the same directions are also shown for comparison. It is apparent from these comparisons that the electronic structures of the $\sqrt{3}\times\sqrt{3}$-Sn and $\sqrt{3}\times\sqrt{3}$-Ga surfaces are very similar to each other except for the presence of the S_1' band for the $\sqrt{3}\times\sqrt{3}$-Sn surface. Actual spectra of the $\sqrt{3}\times\sqrt{3}$-Sn and the three $\sqrt{3}\times\sqrt{3}$-M surfaces are also very similar to each other except for the S_1 and S_1' bands near the Fermi level for the $\sqrt{3}\times\sqrt{3}$-Sn surface. The distinction of the S_1' band from the S_1 band is described later. The E_b vs $k_\parallel$ diagrams below ~2 eV are also similar to those for the Si(111) 7×7 surface. This implies that the electronic structures below ~2 eV are mostly bulk in origin.[1,3] It is clearly seen in Figs. 2 and 3 that the SS bands S_1', S_2, and S_3 disperse in accordance with the periodicity of the $\sqrt{3}\times\sqrt{3}$ SBZ.

In Fig. 4, the dispersions of the SS bands along the $\bar{\Gamma}$-$\bar{M}$-$\bar{\Gamma}$ and $\bar{\Gamma}$-$\bar{K}$-$\bar{M}$ directions are summarized for the $\sqrt{3}\times\sqrt{3}$-Sn surface (a), and for the three $\sqrt{3}\times\sqrt{3}$-M sur-

 © 1986 The American Physical Society

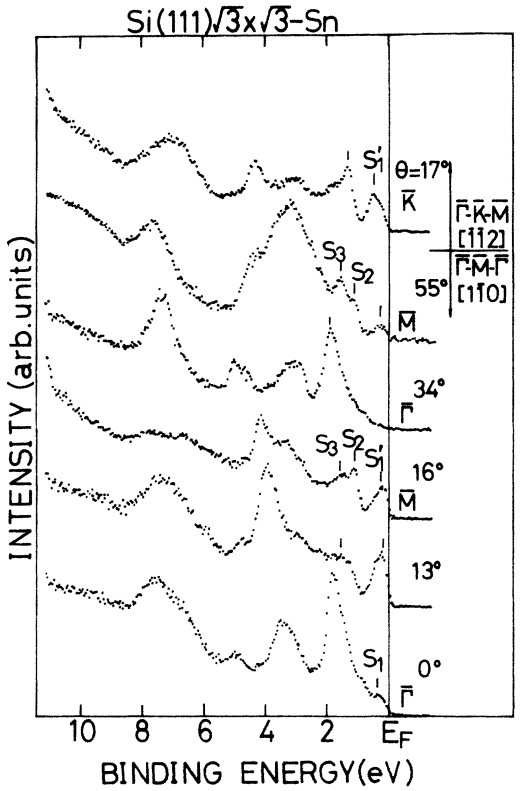

FIG. 1. ARUPS spectra of the Si(111) $\sqrt{3}\times\sqrt{3}$-Sn surface. Polar angle, θ, of electron emission is changed along the $\bar{\Gamma}$-$\bar{M}$-$\bar{\Gamma}$ and $\bar{\Gamma}$-$\bar{K}$-$\bar{M}$ directions of the $\sqrt{3}\times\sqrt{3}$ SBZ. Unpolarized He I light is incident at $\theta\approx -45°$. Symmetric points of the $\sqrt{3}\times\sqrt{3}$ SBZ are indicated. The origin of the binding energy is the Fermi level determined from that of a Ta sample holder.

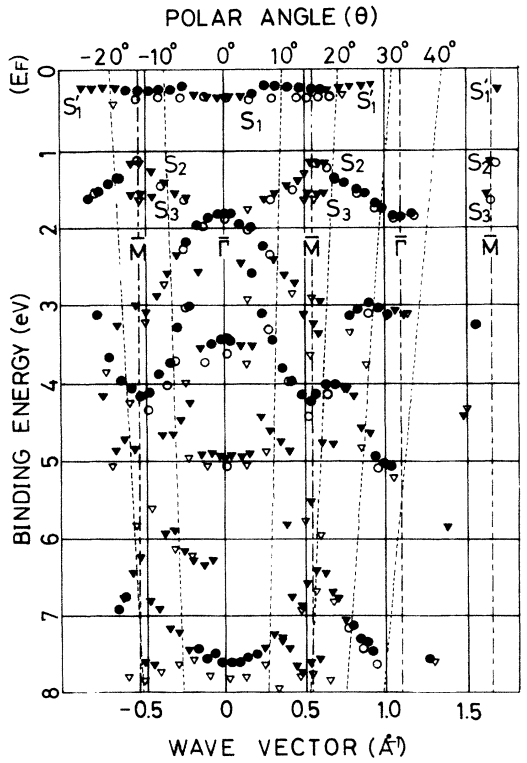

FIG. 2. E_b vs $k_\parallel$ diagram for the Si(111) $\sqrt{3}\times\sqrt{3}$-Sn surface (filled symbols) as compared with that for the Si(111) $\sqrt{3}\times\sqrt{3}$-Ga surface (Ref. 3) (open symbols) along $\bar{\Gamma}$-$\bar{M}$-$\bar{\Gamma}$ direction. Circles are strong or sharp peaks and triangles are weak or broad structures in actual ARUPS spectra.

faces (b)–(d). It is clear from the comparison that the S_2 and S_3 bands for the $\sqrt{3}\times\sqrt{3}$-Sn surface disperse very similarly to those for the $\sqrt{3}\times\sqrt{3}$-M surfaces. The separation between the S_2 and S_3 bands for all the surfaces is not visible in the direction between $\bar{\Gamma}$ and $\bar{K}$ in Fig. 4, for which the two bands are probably very close. The separation is visible near the $\bar{M}$ points along the $\bar{\Gamma}$-$\bar{M}$ direction for all the surfaces. It is also visible near the $\bar{M}$ points along the $\bar{\Gamma}$-$\bar{K}$-$\bar{M}$ direction for the $\sqrt{3}\times\sqrt{3}$-Ga and $\sqrt{3}\times\sqrt{3}$-In surfaces.

It has been shown that the S_1 band is extrinsic to the $\sqrt{3}\times\sqrt{3}$-M surfaces.[1,3] This extrinsic S_1 band is indicated by open circles in Fig. 4 to distinguish it from the intrinsic SS bands. It is also found for the $\sqrt{3}\times\sqrt{3}$-Sn surface that the S_1 band is seen only at smaller polar angles ($\lesssim 8°$), and overlaps with the new band S_1' (intrinsic to the $\sqrt{3}\times\sqrt{3}$-Sn surface, as explained below) around the midpoints of the $\bar{\Gamma}$-$\bar{M}$ and $\bar{\Gamma}$-$\bar{K}$ directions of the $\sqrt{3}\times\sqrt{3}$ SBZ as seen in Fig. 4(a).

In other studies, we examined the coverage dependence of the ARUPS spectra for the $\sqrt{3}\times\sqrt{3}$-Al,[1] -Ga,[3] and -In (Ref. 6) surfaces in order to characterize the S_1 band. It was observed that the intensities of the S_1 band for these three surfaces are rather high at lower coverage at small polar angles ($\theta\lesssim 18°$) but become weaker as $\sqrt{3}\times\sqrt{3}$ domains spread wider with an increase in coverage. The same sort of coverage dependence is observed for the S_1 band of the $\sqrt{3}\times\sqrt{3}$-Sn surface this time. However, for the S_1' band of the Sn overlayer, the intensity does not change very much with an increase in coverage and remains rather strong until the $\sqrt{3}\times\sqrt{3}$ phase changes completely to the $2\sqrt{3}\times 2\sqrt{3}$ phase which is the second phase at higher coverage. These facts give evidence for the intrinsic nature of the S_1' band and the extrinsic nature of the S_1 band.

The S_1' band shows a sharp Fermi edge for the spectra at $\theta=13°$ and 16° in Fig. 1. This is also the case for the spectra at $8°\lesssim\theta\lesssim 17°$ along the $\bar{\Gamma}$-$\bar{M}$ direction and at $7°\lesssim\theta\lesssim 13°$ along the $\bar{\Gamma}$-$\bar{K}$ direction as judged from Figs. 2 and 3. This means that the $\sqrt{3}\times\sqrt{3}$-Sn surface is metallic. Along the $\bar{\Gamma}$-$\bar{K}$ direction, the S_1' band shows clear dispersion, where the binding energy becomes largest at the $\bar{K}$ points as seen in Fig. 3. Also in Fig. 2, the S_1' band can be observed again at $\bar{M}$ point ($\theta=55°$) of the second SBZ in contrast to the S_1 band, which is not observable in the second SBZ. This is another reason why we distinguish the two and assign the S_1 band as extrinsic and the S_1' band as intrinsic to the $\sqrt{3}\times\sqrt{3}$ surface. This is because the extrinsic S_1 band is expected to distribute all over the SBZ without dispersion, but it is visible only at small θ's.

The close similarity of the dispersions of the S_2 and S_3 bands between the $\sqrt{3}\times\sqrt{3}$-Sn and the $\sqrt{3}\times\sqrt{3}$-M surfaces suggests an equivalent surface atomic geometry for the $\sqrt{3}\times\sqrt{3}$-Sn surface to those for the $\sqrt{3}\times\sqrt{3}$-M sur-

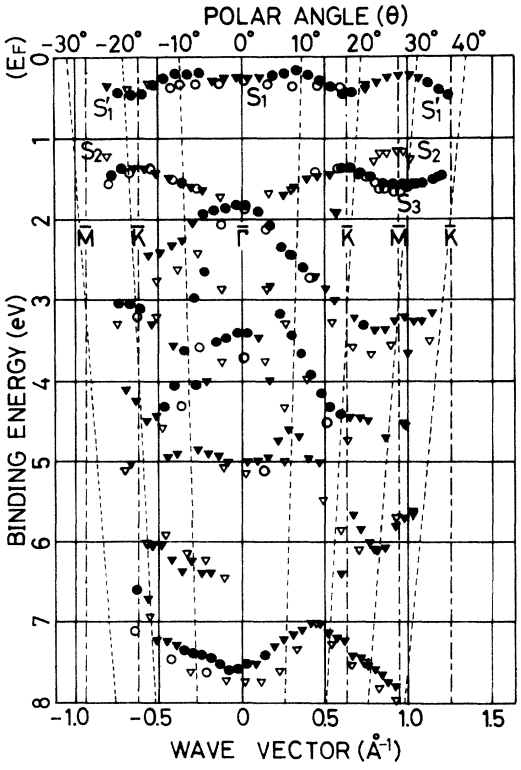

FIG. 3. As in Fig. 2 but along the $\bar{\Gamma}$-$\bar{K}$-$\bar{M}$ direction.

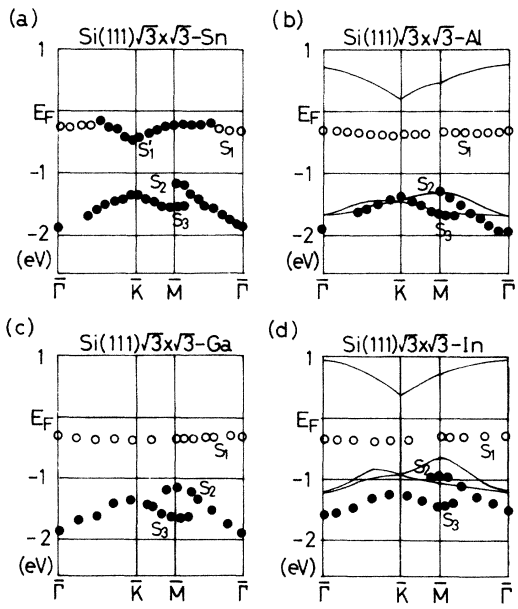

FIG. 4. (a) Summary of surface-state dispersions for the $\sqrt{3}\times\sqrt{3}$-Sn surface. Filled and open circles are surface states intrinsic and extrinsic to the $\sqrt{3}\times\sqrt{3}$ surface, respectively. (b) As in (a) but for the $\sqrt{3}\times\sqrt{3}$-Al surface (Ref. 1). Solid curves are theoretical calculation by Northrup (Ref. 7) for the T_4 model. The value of $E_F - E_V \approx 0.8$ eV is assumed as in Ref. 7. (c) As in (a) but for the $\sqrt{3}\times\sqrt{3}$-Ga surface (Ref. 3). (d) As in (a) but for the $\sqrt{3}\times\sqrt{3}$-In surface (Ref. 6). Solid curves are theoretical calculation in Ref. 5 for the H_3 model. The value of $E_F - E_V \approx 0.5$ eV is assumed, as in Ref. 4.

faces. However, to proceed with this idea, we need to find the origin of the additional metallic S_1' band, which is the following.

The calculated SS dispersions of the $\sqrt{3}\times\sqrt{3}$-Al (Ref. 7) and $\sqrt{3}\times\sqrt{3}$-In (Refs. 4 and 5) surfaces are shown with solid lines in Figs. 4(b) and 4(d) together with our experimental results. These calculations have been carried out for both the T_4 and H_3 models by Northrup. H_3 is a model in which there is $\frac{1}{3}$ ML of adatoms in the threefold-hollow sites of Si(111) substrate and with no second layer of Si atoms underneath. T_4 is a model in which $\frac{1}{3}$ ML of adatoms are in the threefold-hollow sites above second-layer Si atoms. The calculated dispersions for the $\sqrt{3}\times\sqrt{3}$-Al and $\sqrt{3}\times\sqrt{3}$-In surfaces shown in Figs. 4(b) and 4(d) are of the T_4 and H_3 models, respectively. As seen in the figures, the calculated bands for both models are essentially similar to each other, but Northrup supported the T_4 model from total energy calculation for both the $\sqrt{3}\times\sqrt{3}$-Al and $\sqrt{3}\times\sqrt{3}$-In surfaces. Comparing the experimental results with theoretical calculations in Fig. 4, the dispersions of S_2 and S_3 bands for the four surfaces qualitatively agree with the calculated ones.

The metallic S_1' band for the $\sqrt{3}\times\sqrt{3}$-Sn surface seems to disperse in accordance with the unoccupied SS bands of the calculations. If the atomic geometry of the $\sqrt{3}\times\sqrt{3}$-Sn surface is the T_4 or H_3 structure, it is reasonable to consider that the unoccupied band for the $\sqrt{3}\times\sqrt{3}$ surface is partially filled, since the Sn atom is a column-IV element and has one more valence electron than the column-III atoms. This partially filled band would result in the metallic S_1' band of the $\sqrt{3}\times\sqrt{3}$-Sn surface. Filling of an antibonding-type orbital would cause weakening of the bond. The $\sqrt{3}\times\sqrt{3}$-Sn surface is, however, very stable up to $\sim 860\,^{\circ}$C.[10] Therefore, the present model needs to be examined further by theory.

In conclusion, we have found that the $\sqrt{3}\times\sqrt{3}$-Sn surface has S_1, S_2, and S_3 SS bands similar to those of the $\sqrt{3}\times\sqrt{3}$-M surfaces. In addition to these bands, the metallic and dispersive S_1' band is present for the $\sqrt{3}\times\sqrt{3}$-Sn surface. The S_2, S_3, and S_1' bands are identified as intrinsic to the $\sqrt{3}\times\sqrt{3}$ surface. Considering the increase in valency of the Sn atom as compared with the column-III atoms, it is tentatively proposed that the atomic geometry of the $\sqrt{3}\times\sqrt{3}$-Sn surface is essentially the same as those of the $\sqrt{3}\times\sqrt{3}$-M surfaces and that the S_1' band of the $\sqrt{3}\times\sqrt{3}$-Sn surface corresponds to the otherwise empty SS bands of the $\sqrt{3}\times\sqrt{3}$-M surfaces.

We thank Dr. S. Suzuki for his invaluable contribution in the construction of our apparatus.

[1]T. Kinoshita, S. Kono, and T. Sagawa, Phys. Rev. B **32**, 2714 (1985).

[2]R. I. G. Uhrberg, G. V. Hansson, J. M. Nicholls, P. E. S. Persson, and S. A. Flodström, Phys. Rev. B **31**, 3805 (1985).

[3]T. Kinoshita, S. Kono, and T. Sagawa, Solid State Commun. **56**, 681 (1985).

[4]J. M. Nicholls, P. Mårtensson, G. V. Hansson, and J. E. Northrup, Phys. Rev. B **32**, 1333 (1985).

[5]G. V. Hansson, J. M. Nicholls, P. Mårtensson, and R. I. G. Uhrberg, Surf. Sci. **168**, 105 (1986).

[6]T. Kinoshita, S. Kono, and T. Sagawa (unpublished).

[7]J. E. Northrup, Phys. Rev. Lett. **53**, 683 (1984).

[8]H. Nagayoshi, in *Dynamical Processes and Ordering on Solid Surfaces,* edited by A. Yoshimori and M. Tsukada, Solid-State Sciences, Vol. 59 (Springer-Verlag, Berlin, 1985), p. 167.

[9]P. J. Estrup and J. Morrison, Surf. Sci. **2**, 465 (1964).

[10]T. Ichikawa, Surf. Sci. **140**, 37 (1984).

[11]Y. Yabuuchi, Ph.D. thesis, Osaka University, Suita, Japan, 1984 (unpublished).